An efficient algorithm for the density-functional theory treatment of dispersion interactions

Jürgen Gräfenstein[1,a] and Dieter Cremer[2]
[1]*Department of Chemistry, University of Gothenburg, S-412 96 Göteborg, Sweden*
[2]*Department of Chemistry and Department of Physics, University of the Pacific, 3601 Pacific Ave., Stockton, California 95211-0110, USA*

(Received 29 August 2008; accepted 10 November 2008; published online 23 March 2009)

The quasi-self-consistent-field dispersion-corrected density-functional theory formalism (QSCF-DC-DFT) is developed and presented as an efficient and reliable scheme for the DFT treatment of van der Waals dispersion complexes, including full geometry optimizations and frequency calculations with analytical energy derivatives in a routine way. For this purpose, the long-range-corrected Perdew–Burke–Ernzerhof exchange functional and the one-parameter progressive correlation functional of Hirao and co-workers are combined with the Andersson–Langreth–Lundqvist (ALL) long-range correlation functional. The time-consuming self-consistent incorporation of the ALL term in the DFT iterations needed for the calculation of forces and force constants is avoided by an *a posteriori* evaluation of the ALL term and its gradient based on an effective partitioning of the coordinate space into global and intramonomer coordinates. QSCF-DC-DFT is substantially faster than SCF-DC-DFT would be. QSCF-DC-DFT is used to explore the potential energy surface (PES) of the benzene dimer. The results for the binding energies and intermolecular distances agree well with coupled-cluster calculations at the complete basis-set limit. We identify 16 stationary points on the PES, which underlines the usefulness of analytical energy gradients for the investigation of the PES. Furthermore, the inclusion of analytically calculated zero point energies reveals that large-amplitude vibrations connect the eight most stable benzene dimer forms and make it difficult to identify a dominating complex form. The tilted T structure and the parallel-displaced sandwich form have the same D_0 value of 2.40 kcal/mol, which agrees perfectly with the experimental value of 2.40 ± 0.40 kcal/mol. © *2009 American Institute of Physics*. [DOI: 10.1063/1.3079822]

I. INTRODUCTION

Noncovalent intermolecular forces of the π-π stacking type play an important role in the structural organization and in physiochemical processes of many supramolecular assemblies, biomolecules, or nanoparticles.[1–12] Best known examples in this connection are the DNA base-pair stacking,[5] host-guest complexation reactions,[6–9] folding of proteins,[1,2] adhesion of carbon nanotubes (CNTs) in rods,[10] or intercalation of drugs into DNA.[11,12] It is one of the major objectives of current computational chemistry to describe π-π stacking interactions correctly and to decrypt the nature of these interactions.[13] A benchmark system in this connection, which has repeatedly been investigated both experimentally[14–22] and computationally is the benzene dimer.[23–47] *Ab initio* investigations in the form of Møller–Plesset perturbation theory and coupled-cluster theory have paved the way for an understanding and accurate description of the most stable benzene dimer forms and the binding energies involved where especially the work of Sherill and co-workers,[26,28,29,31,35] that of Tsuzuki *et al.*,[23–25,30] and the more recent works by Hill *et al.*,[34] DiStasio *et al.*,[38] Hobza and co-workers,[36,37,39] Janowski and Pulay,[40] and Lee *et al.*[44] have to be mentioned. Symmetry-adapted perturbation theory (SAPT) has helped understand which of the benzene dimer forms is stabilized more by dispersion (π-π stacking), induction, or electrostatic forces.[31,33]

However, extensive CCSD(T) or even CCSD(TQ) calculations for a relatively small system such as the benzene dimer are difficult to carry out with today's computer hardware. A complete study of the benzene dimer involves the determination of all stationary points of indices 0 and 1 on its potential energy surface (PES), routine geometry optimizations, vibrational frequency calculations to characterize the stationary points identified and to obtain thermochemical properties, or carrying out of molecular dynamics calculations to assess the dynamical behavior of the benzene dimer (large-amplitude vibrations, rapid rearrangements, etc.). The task of describing π-π stacking interactions in the naphthalene, anthracene, coronene, or graphene dimers is completely out of the range of an accurate coupled-cluster investigation. Hence, a much cheaper but nevertheless reliable quantum chemical method is needed for this purpose. This method must be able to describe both monomers and dimers correctly and it must include the routine calculation of the analytical energy gradient and the Hessian matrix. Such a method could be density-functional theory (DFT), which has

[a]Electronic mail: jurgen.grafenstein@chem.gu.se.

been emphasized in literally dozens of investigations that focus on the efficient and reliable calculation of π-π stacking and dispersion forces in general.[48–81]

The deficiencies of DFT when describing dispersion interactions have been traced back to a lack of long-range (LR) electron correlation in approximate exchange-correlation (XC) functionals.[82–84] The last ten years have seen numerous and partly impressive attempts to improve DFT for the correct description of dispersion forces and the reliable calculation of van der Waals (vdW) complexes. These attempts can be ordered in five different groups:

(i) Extension of DFT by constructing dispersion adjusted Kohn–Sham (KS) methods (ρ-based methods):[48–61] In this connection the work by Langreth and co-workers leading to vdW-DFT,[49,53–58] the Andersson–Langreth-Lundqvist (ALL),[49] and Dion–Rydberg–Schröder–Langreth–Lundqvist (DRSLL) dispersion-correction (DC) functionals[53,54] have to be mentioned; Hirao and co-workers used the ALL functional and combined it with a range-separated X functional to obtain an efficient approach for the description of vdW complexes.[32,50–52] This work was possible due to the pioneering work on the development of range-separated DFT functionals[85–87] that originally did not focus on the DFT dispersion problem.[60,61]

(ii) Improvement of XC functionals for dispersion:[65–70] Although this seems to be the direct way of improving DFT, it turned out that it is rather difficult to design generalized gradient approximation (GGA) or meta-GGA functionals that accurately describe dispersion forces. Attempts by Xu and Goddard,[65] Zhao *et al.*,[66,67,70] Schweigert *et al.*,[68] and Gritsenko and Baerends[69] have to be mentioned.

(iii) Combining DFT with symmetry-adapted perturbation theory [SAPT(DFT)]: An approach to use KS orbitals and orbital energies from a DFT calculation to carry out a SAPT description of vdW complexes was advocated in Refs. 33 and 71–74. This has led to the most advanced description of the parts of the PES of the benzene dimer. Since SAPT has also been essential when explaining interactions stabilizing the benzene dimer, the SAPT(DFT) method, although not a genuine DFT approach, is mentioned here.

(iv) Hybrid methods of the DFT-molecular mechanics (MM) type [not to be confused with the DFT/MM methods that are used in quantum mechanics in quantum mechanics (QM)/MM]:[76–81] In this approach, DFT is empirically corrected by a London-type dispersion term (DFT-D, DFT with dispersion). DFT-D has been early suggested and developed to an efficient computational scheme by Grimme *et al.*[41,46,79,80] The correction term is formed by a sum over all pair interactions and in order to avoid double counting of electron correlation as well as singularity problems multiplied by a damping function. Despite its efficiency DFT-D is problematic for two reasons: (1) It is assumed that the dispersion interaction between the atom pairs is additive. This additivity cannot be taken for granted, as was shown by Tkatchenko and von Lilienfeld.[88] (2) The dispersion interaction requires extensive parametrization considering that one should also distinguish the various hybridization states of an atom (sp^3- and sp^2-hybridized carbon possess different dispersion forces[78]). In this way, DFT-D may be more useful for semiempirical methods such as tight-binding DFT,[76] whereas its use in the DFT framework has to be questioned because it excludes the assessment of collective QM effects.

(v) Hybrid methods of the DFT–*ab initio* type: Grimme combined BLYP with MP2 (leading to B2-PLYP) and obtained an improved description of vdW complexes at the price of losing the simplicity of the KS DFT approach.[89] von Lilienfeld *et al.*[90] added an atomic-centered nonlocal attractive pseudopotential to the nuclear potential of each nucleus; this idea has recently been adapted by DiLabio.[91] Nachtigall and co-workers[47,75] solved the DFT dispersion problem by determining CCSD(T) correction energies for reference systems of moderate size in a clever way and then using CCSD(T) corrections for the actual target systems. Their DFT/CCSD(T) approach combines high accuracy with costs comparable to those of standard DFT calculations. However, the range of applicability is limited by the class of reference systems for which benchmark calculations are available and readjustment of CCSD(T) corrections has to be done for each new XC functional and basis set.

(vi) Engel *et al.*[92] combined the optimized potential method (OPM)[93] for the exchange energy with KS perturbation theory[94] to correctly treat dispersion interactions. Tests for He_2 and Ne_2 indicate that the resulting FC2 (exact exchange with second order correlation)-OPM algorithm correctly reproduces the R^{-6} behavior of the dispersion energy and provides a semiquantitative description of the complexes, with the D_e values being overestimated by 50% for He_2 and 120% for Ne_2.

Most of methods (i)–(vi) have been tested for the benzene dimer and some of them have led to impressive results largely reproducing high level *ab initio* geometries and relative energies. Despite the success of the dispersion-improved DFT methods, there are still open questions, which prevent from stating that the DFT dispersion problem has been solved once and forever.

In this work, we reformulate the criteria for dispersion-improved DFT. For reasons indicated above and worked out in more detail in Sec. II, we follow approach (i) and use the DC functional ALL (Ref. 49) to develop a very accurate and cost-efficient DFT method for dispersion. For this purpose, we take advantage of the previous work carried out by Hirao and co-workers[32,50–52] to adjust the XC functional to the DC-ALL functional. However, we will make some essential changes in the functional setup to obtain a dispersion-improved DFT approach for routine calculations. In the following section, our new methodological approach will be described. Application of the new approach to the benzene

dimer will be presented to demonstrate its applicability and feasibility for π-π stacking systems. Conclusions and an outlook with regard to future applications of our new method will be discussed in the last section of this work.

II. METHODOLOGY

An efficient and reliable dispersion-improved DFT method has to fulfill the following criteria: (1) general applicability; (2) the approach should stay within the KS-DFT frame (no hybrid methods), (3) asymptotic R^{-6} behavior of LR correlation should be fulfilled; (4) the method must be size extensive; (5) double counting of correlation must be avoided; (6) analytical energy derivatives (gradient and Hessian matrix) must be available for routine calculations; (7) the method must be cost effective (not much more expensive than KS-DFT).

The criterion of general applicability implies that vdW complexes of different natures must be described in a balanced way, which in turn implies that exchange repulsion, electrostatic, inductive, and dispersion interactions are described with the same or at least similar accuracy. By requiring that the LR-correlation effects are described correctly, expectations with regard to the accuracy of a dispersion-improved DFT method are specified: The accuracy should be definitely better than MP2 (Ref. 95) or Grimme's spin component scaling MP2 (Ref. 96) method.[13,43] However, it would be misleading to require that dispersion-improved DFT should exactly reproduce CCSD(T)/complete basis-set (CBS) results [as done for DFT/CCSD(T) (Refs. 47 and 75)] because it is not clear whether the latter are absolutely reliable. For example, Hopkins and Tschumper[97] found that the inclusion of quadruples as in CCSD(TQ) leads to a correction of 0.2 kcal/mol in the case of the furan dimer and an estimated 0.1 kcal/mol for systems comparable to the benzene dimer. However, more recent studies by Hobza[98] determined the contribution of Q effects in CCSD(TQ) to be smaller than 0.05 kcal/mol. Hence, one should require that general trends in CCSD(T) vdW binding energies are reproduced without the need of an exact (0.01 kcal/mol) reproduction of the CCSD(T) values. A possible double counting of LR correlation may violate the size-extensiveness requirement, which in turn would lead to unreliable vdW binding energies. Most important is the routine calculation of geometry, vibrational frequencies, zero point energy (ZPE), and temperature corrections with the help of analytical energy derivatives, which is a significant problem for some of the methods described in the introduction. The latter criterion is of course tightly connected to the required cost effectiveness of the method. This excludes any *ab initio*-based corrections. Apart from this, one has to consider that KS-DFT calculations of vdW complexes are normally somewhat more costly than the calculation of the monomers (apart from the doubling of the number of basis functions) because of slow convergence of both SCF (caused by the needed diffuse functions) and geometry optimization (caused by the flat PES). A cost effective dispersion-improved DFT method should therefore stay within about +30% of the computation time of a normal KS-DFT calculation of the same vdW complex.

A prospective route for the description of dispersion within the normal KS-DFT has been followed in Refs. 49 and 53–58 wherein vdW-DFT was developed. In this approach, the dispersion energy is covered by an extra term in the correlation functional. This term has the form of a double integral in space. In the original ALL functional,[49] the two integrations have to be performed over one of the fragments each; thus the system has to be decomposed explicitly into two fragments. For the more recent DRSLL functional,[53–55] both integrations stretch over the whole space; thus no assumption needs to be made on the fragment structure of the system.

The vdW-DFT approach leads to fairly accurate descriptions of dispersion interactions at costs comparable to standard DFT calculations as has been demonstrated for typical π-π stacking problems.[56–58] Moreover, the approach is parameter-free and not biased toward a particular class of systems. We therefore use vdW-DFT for a reliable description of π-π stacking. However, the standard vdW-DFT method suffers from an important limitation: The dispersion term is evaluated non-self-consistently, i.e., it is calculated *a posteriori* and added to the standard DFT energy. Thonhauser *et al.*[55] developed and implemented a self-consistent version of the DRSLL functional and confirmed that the difference between the results from self-consistent and *a posteriori* vdW-DFT calculations is negligible. Nevertheless, the calculation of analytical derivatives by standard methods requires a self-consistent solution of the underlying KS equations. Calculation of the DC term in a self-consistent fashion increases the computational cost in three ways: (i) In addition to the DC correlation energy, the DC correlation potential has to be calculated. (ii) The DC term has to be calculated in every iteration step rather than just once at the end of the calculation. (iii) Obtaining self-consistency may require additional SCF iterations beyond those needed for the corresponding standard KS-DFT calculation.

Vydrov *et al.*,[59] who adapted the algorithm from Ref. 55 for Gaussian basis functions, presented benchmark calculations suggesting that a self-consistent calculation of the DC term may increase computational cost by about a factor of 10, which suggests limited applicability of this approach to larger systems such as graphene or CNTs. In contrast, a non-self-consistent calculation of the DC term implies only a minor increase in computing time.[55] In this situation, we sought a way of calculating analytical forces and force constants at a sufficient level of accuracy without the need of incorporating the dispersion term self-consistently. This has led to the development of the *quasi-self-consistent-field dispersion-corrected-DFT* (QSCF-DC-DFT) method presented in the current paper.

A prerequisite for the QSCF-DC-DFT approach is that the dispersion term exclusively contains the LR dispersion energy. This is the case for the original ALL functional[49] but not for the DRSLL functional, which contains all nonlocal corrections to the correlation energy including the gradient corrections usually covered by GGA correlation functionals[53,54] Therefore, we use the ALL LR-correlation functional for describing dispersion interactions. According to Hirao and co-workers[50,51] the proper implementation of

DC-DFT requires that the standard exchange+short-range (SR) correlation part of the XC functional must neither result in an artificial bonding nor a LR repulsion between the fragments of the complex. Most standard functionals do not fulfill this requirement: Slater exchange predicts an artificial binding; the same, though less distinct, applies to the Perdew–Burke–Ernzerhof (PBE) exchange functional.[99] Becke exchange,[100] in contrast, gives an LR repulsion between the fragments. The popular LYP correlation functional[101] leads to an artificial binding as well. The artificial attraction or repulsion may be of the same order of magnitude as the dispersion energy to be described. Consequently, simply adding the ALL or DRSLL term to a standard XC functional may result in a description of vdW complexes that is wrong even qualitatively.

Exact [Hartree–Fock (HF)] exchange does not suffer from artificial attraction or repulsion. We therefore follow Hirao and co-workers[50,51] and use HF exchange to describe the LR part of the exchange energy, whereas a SR DFT functional is used to describe SR exchange energy contributions. Using a DFT expression for SR exchange improves accuracy by allowing error compensation between the exchange and SR-correlation terms. For the SR-correlation part, we use the one-parameter progressive (OP) functional,[102] which describes weakly bound complexes in a balanced way. In Refs. 53–58, PBE functional as revised by Zhang and Yang[103] (revPBE) for the exchange term was used. The revPBE term indeed shows neither artificial attraction nor LR repulsion for weakly bound complexes;[53] however, Puzder *et al.*[56] found that the use of revPBE exchange results in a systematic overestimation of bond distances, which we could confirm in test calculations. Therefore, we kept the PBE exchange functional for SR exchange, especially since an elaborate parametrization for this functional is available.[104] In test calculations, we could confirm that within the combination SR-DFT+LR-HF for the exchange term and the OP functional for correlation, use of the SR-PBE functional is appropriate, which is in line with the observations of Hirao and co-workers.[50,51] Hence, the total XC functional takes the form

$$E_{\mathrm{XC}} = E_{\mathrm{X,PBE}}^{\mathrm{SR}} + E_{\mathrm{X,HF}}^{\mathrm{LR}} + E_{\mathrm{C,OP}} + E_{\mathrm{C,ALL}}, \tag{1}$$

where the indices X and C refer to exchange and correlation, respectively; our approach may thus be described as SR-PBE+LR-HF+OP+ALL. In the next section, we will show how analytical energy gradient and Hessian matrix can be determined for this approach at relatively low cost.

A. Theory of the quasi-self-consistent-field dispersion-corrected-DFT method

In the formalism developed by ALL,[49] the dispersion interaction between two molecular fragments A and B is accounted for by an explicit term $E_{\mathrm{C,DC}}$, which has the form

$$E_{\mathrm{C,DC}} = \frac{1}{2}\int_{V_A} d^3r_1 \int_{V_B} d^3r_2 W[\rho_A(\mathbf{r}_1), \nabla\rho_A(\mathbf{r}_1), \rho_B(\mathbf{r}_2), \nabla\rho_B(\mathbf{r}_2)] \times \psi(|\mathbf{r}_1 - \mathbf{r}_2|). \tag{2}$$

Here, V_A and V_B are the volumes containing fragments A and B and ρ_A and ρ_B the densities related to the fragments. Hartree atomic units are used throughout the paper. In Eq. (2) and in the following, we use the index DC rather than ALL to indicate that the algorithm to be derived is not tied to the specific form of the ALL functional. W is a kernel function depending on the densities ρ_A and ρ_B arising from fragments A and B and their gradients $\nabla\rho_A$ and $\nabla\rho_B$ at $\mathbf{r}_1$ and $\mathbf{r}_2$, respectively. The full expression for W is given in Sec. II B. In the original work leading to the ALL functional,[49] $\psi(r)$ is set equal to r^{-6}. For the purpose of avoiding a double counting of electron correlation effects and avoiding numerical problems for $r \to 0$, Hirao and co-workers[50,51] suggested to choose $\psi(r)$ as

$$\psi(r) = h(r) r^{-6}, \tag{3}$$

where h is a cutoff function chosen such that $\psi(r) \to 0$ for $r \to 0$, whereas $h \to 1$ for $r \to \infty$.

In principle, the term $E_{\mathrm{C,DC}}$ can be incorporated into the KS formalism, i.e., the KS equations for the energy functional including $E_{\mathrm{C,DC}}$ can be solved self-consistently. Investigations by Thonhauser *et al.*[55] for the DRSLL functional[53,54] have shown that the impact of dispersion on the density is rather small and that $E_{\mathrm{C,DC}}$ to a good accuracy can be evaluated *a posteriori* with the density from a conventional DFT calculation, which reduces computational cost substantially. However, an *a posteriori* evaluation of $E_{\mathrm{C,DC}}$ does not allow to calculate energy gradients and force constants by standard techniques. In the following, we present an algorithm that makes it possible to determine the contributions of $E_{\mathrm{C,DC}}$ to forces and force constants at reasonable accuracy without the need to solve the KS-ALL equations self-consistently. In our approach, the contributions to forces and force constants arising from the conventional XC contributions (i.e., exchange and SR correlation) are determined in the usual way. The contributions from $E_{\mathrm{C,DC}}$ are calculated explicitly and will be treated technically in the same way as, e.g., the contributions from the nucleus-nucleus repulsion or a possible pseudopotential term.

The calculation of analytic energy derivatives requires that $E_{\mathrm{C,DC}}$ in dependence of the nuclear displacements $\underline{x} = (x_i, i = 1, \ldots, 3N)$ (N is the number of nuclei in the molecule) is represented in the form

$$E_{\mathrm{C,DC}}(\underline{x}) = E_0 + \sum_i F_i x_i + \frac{1}{2}\sum_{i,k} K_{ik} x_i x_k, \tag{4a}$$

where

$$E_0 = E_{\mathrm{C,DC}}(\underline{x} = \underline{0}), \tag{4b}$$

$$F_i = \left(\frac{\partial E_{\mathrm{C,DC}}}{\partial x_i}\right)_{\underline{x}=\underline{0}}, \tag{4c}$$

$$K_{ik} = \left(\frac{\partial^2 E_{\mathrm{C,DC}}}{\partial x_i\, \partial x_k}\right)_{\underline{x}=\underline{0}}. \tag{4d}$$

Note that we suppress the subscript DC for E_0, F_i, and K_{ik}; i.e., E_0, F_i, and K_{ik} refer to $E_{\mathrm{C,DC}}$ rather than the total energy. Also, note the sign convention we apply for F (dropping the minus sign).

Our approach in determining F_i and K_{ik} is based on two assumptions:

(a) For a small displacement moving A and B rigidly as a whole or against each other (*global displacement*), the densities ρ_A and ρ_B basically follow the displacements of A and B. If the displacement for the two fragments can be described by coordinate transformations $\mathbf{r}_1 \rightarrow \mathbf{r}_1' = \mathbf{r}_1 + \Delta\mathbf{r}_1$ and $\mathbf{r}_2 \rightarrow \mathbf{r}_2' = \mathbf{r}_2 + \Delta\mathbf{r}_2$, we can perform the corresponding coordinate transformation in Eq. (2) and represent the new value of $E_{\mathrm{C,DC}}$ as

$$E_{\mathrm{C,DC}} \rightarrow E'_{\mathrm{C,DC}} = \frac{1}{2}\int_{V_A} d^3r_1' \int_{V_B} d^3r_2' K[\rho_A(\mathbf{r}_1'), \nabla\rho_A(\mathbf{r}_1'), \rho_B(\mathbf{r}_2'), \nabla\rho_B(\mathbf{r}_2')]\psi(|\mathbf{r}_1 - \mathbf{r}_2 + \Delta\mathbf{r}_1 - \Delta\mathbf{r}_2|). \tag{5}$$

Equation (5) shows that $E'_{\mathrm{C,DC}}$ can be calculated explicitly from the original densities ρ_A and ρ_B. In the special case of an overall rigid displacement of A and B, $E_{\mathrm{C,DC}}$ remains unchanged.

Assumption (a) makes it possible to calculate the force and torque the fragments exert on each other as a whole, as well as the corresponding force constants, but not the forces on the individual nuclei. For the purpose of decomposing forces and torques into contributions from the individual nuclei we have to add a second assumption.

(b) For small *intrafragment displacements*, i.e., displacements within the fragments that do not involve any global displacement, we assume that $E_{\mathrm{C,DC}}$ does not change. This assumption is reasonable for two reasons: (i) The ALL expression has been set up to determine the LR-correlation interactions between rather than within the fragments. (ii) The energy changes for intrafragment displacements are dominated by strong (covalent or ionic) chemical bonds, which confine intrafragment geometry changes to a narrow range. Thus, the DC energy plays only a small role for the intrafragment geometry and energetics. (If this were not the case, it would not be defendable to treat the fragments with conventional KS-DFT.) Accordingly, we assume that all DC energy gradients and all second DC energy derivatives involving at least one intrafragment displacement are equal to zero.

Assumptions (a) and (b) determine the change of $E_{\mathrm{C,DC}}$ for any displacement $\underline{x}$ and thus make it possible to determine the F_i and K_{ik} in the following way:

(1) Define a set of $3N$ collective displacements of the nuclei in the way that each of them describes either a global or an intrafragment displacement.

The collective displacements are described by coordinates ξ_α ($\alpha = 1, \ldots, 3N$), which are related to the x_i up to second order by

$$x_i = \sum_\alpha \underbrace{\left(\frac{\partial x_i}{\partial \xi_\alpha}\right)_{\underline{x}=\underline{0}}}_{=C_{i\alpha}} \xi_\alpha + \frac{1}{2}\sum_{\alpha\beta} \underbrace{\left(\frac{\partial^2 x_i}{\partial \xi_\alpha \partial \xi_\beta}\right)_{\underline{x}=\underline{0}}}_{=D_{i\alpha\beta}} \xi_\alpha \xi_\beta \tag{6}$$

or conversely (again to second order)

$$\xi_\alpha = \sum_i \underbrace{\left(\frac{\partial \xi_\alpha}{\partial x_i}\right)_{\underline{\xi}=\underline{0}}}_{=c_{\alpha i}} x_i + \frac{1}{2}\sum_{ik} \underbrace{\left(\frac{\partial^2 \xi_\alpha}{\partial x_i \partial x_k}\right)_{\underline{\xi}=\underline{0}}}_{=d_{\alpha ik}} x_i x_k. \tag{7}$$

In Eq. (6), the $C_{i\alpha}$ describe the first order motion of the nuclei for the collective displacement ξ_α, e.g., a translation, rotation, or vibration. The $D_{i\alpha\alpha'}$ reflect the possible curvilinear character of the collective displacements. We note in this connection that the expansion up to second order is necessary for the calculation of force constants. In the following, the sets of ξ_α describing global or intrafragment displacements will be denoted by G and I, respectively. We note that the matrix $c_{\alpha i}$ is analogous to the B matrix used in molecular spectroscopy.[105] These collective displacements are similar to internal coordinates apart from the fact that translations and rotations of the molecule as a whole are not excluded at this stage.

(2) Determine the forces and force constants in terms of the coordinates ξ_α,

$$\bar{F}_\alpha = \left(\frac{\partial E_{\mathrm{C,DC}}}{\partial \xi_\alpha}\right)_{\underline{\xi}=\underline{0}}, \tag{8a}$$

$$\bar{K}_{\alpha\beta} = \left(\frac{\partial E_{\mathrm{C,DC}}}{\partial \xi_\alpha \partial \xi_\beta}\right)_{\underline{\xi}=\underline{0}}, \tag{8b}$$

where the overlined quantities refer to global displacement variables. For $\alpha, \alpha' \in G$, this calculation is done based on Eq. (2); for $\alpha \in I$ or $\alpha' \in I$, the corresponding $\bar{F}_\alpha$ and $\bar{K}_{\alpha\beta}$ are set to zero.

(3) With the help of Eq. (7), transform the $\bar{F}_\alpha$ and $\bar{K}_{\alpha\beta}$ back to the F_i and K_{ik}:

$$F_i = \sum_\alpha^G c_{\alpha i}\bar{F}_\alpha, \tag{9a}$$

$$K_{ik} = \sum_\alpha^G d_{\alpha ik}\bar{F}_\alpha + \sum_{\alpha\beta}^G c_{\alpha i}c_{\beta k}\bar{K}_{\alpha\beta}. \tag{9b}$$

Here, the $c_{\alpha i}$ and $d_{\alpha ik}$ are given by

$$c_{\alpha i} = \sum_{\alpha'}^{G+I} (g^{-1})_{\alpha\alpha'} C_{i\alpha'}, \tag{10a}$$

$$d_{\alpha ik} = -\sum_{\alpha'}^{G+I} (g^{-1})_{\alpha\alpha'} \sum_{\beta\beta'}^{G+I} \Gamma_{\beta\beta',\alpha'} c_{\beta i} c_{\beta' k}, \tag{10b}$$

where

$$g_{\alpha\alpha'} = \sum_i C_{i\alpha} C_{i\alpha'} \tag{11}$$

is the metric tensor for the curvilinear coordinates ξ_α in the $3N$-dimensional space and

$$\Gamma_{\beta\beta',\alpha'} = \sum_j C_{j\alpha'} D_{j\beta\beta'} \tag{12}$$

are Christoffel symbols. (Note that we do not use covariant/contravariant notation or the Einstein convention in this presentation.) The matrix g^{-1} is similar to Wilson's G matrix,[105] except that we do not use mass-weighted coordinates.

In the form given in Eqs. (9a), (9b), (10a), (10b), (11), and (12), the F_i and K_{ik} depend on the definition of the intrafragment displacements via expressions (10a) and (10b) for the $c_{\alpha i}$ and $d_{\alpha ik}$, even though these displacements are assumed not to affect $E_{\mathrm{C,DC}}$. This is plausible because assumption (b) will hold only if the coordinates $\alpha \in I$ are chosen properly, i.e., do not contain any components of the global displacements. Thus, to employ Eqs. (9a), (9b), (10a), (10b), (11), and (12) one has to explicitly define a set of intrafragment displacements and make sure that these displacements have exclusively intrafragment character up to second order in the ξ_α. We avoid this step by determining the $c_{\alpha i}$, $d_{\alpha ik}$ $(\alpha \in G)$ in a different way based on the following reasoning.

If the coordinates with $\alpha \in I$ describe intrafragment displacements only, the full information on the global displacements must be incorporated into the ξ_α with $\alpha \in G$. This means that if we try to approximate a given displacement $\underline{x}$, which may contain both G and I contributions by a purely global displacement $\underline{\tilde{x}}$ given by

$$\tilde{x}_i = \sum_\alpha^G C_{i\alpha} \tilde{\xi}_\alpha + \frac{1}{2} \sum_{\alpha\beta}^G D_{i\alpha\beta} \tilde{\xi}_\alpha \tilde{\xi}_\beta, \tag{13}$$

where the $\tilde{\xi}_\alpha$ are chosen such that

$$\sum_i (x_i - \tilde{x}_i)^2 \to \min, \tag{14}$$

it should hold that

$$\tilde{\xi}_\alpha = \xi_\alpha \quad \text{for} \quad \alpha \in G, \tag{15}$$

i.e., adding the I displacements should not affect the coordinates for the G displacements. That means that we can determine the relationship between the x_i and the ξ_α, $\alpha \in G$, by performing the minimization in Eq. (14) directly. Up to second order, we obtain

$$c_{\alpha i} = \sum_{\alpha'}^G (g_G^{-1})_{\alpha\alpha'} \sum_i C_{i\alpha'}, \tag{16a}$$

$$d_{\alpha ik} = \sum_{\alpha'}^G (g_G^{-1})_{\alpha\alpha'} \left[\sum_\beta^G (c_{\beta i} D_{k\alpha'\beta} + c_{\beta k} D_{i\alpha'\beta}) - \sum_{\beta\beta'}^G (\Gamma_{\beta\beta',\alpha'} + \Gamma_{\beta\alpha',\beta'} + \Gamma_{\beta'\alpha,\beta}) c_{\beta i} c_{\beta' k} \right]. \tag{16b}$$

Here, g_G is the submatrix of g in the subspace of G displacements. Equation (16b) can be simplified using the fact that the $C_{i\alpha}$ form a complete set of vectors in the $3N$-dimensional space of individual displacements; hence

$$\sum_\alpha^{G+I} C_{i\alpha} c_{\alpha k} = \delta_{ik}. \tag{17}$$

Equation (17) implies that the $D_{i\alpha\alpha'}$ can be expanded into the $C_{i\alpha}$ according to

$$D_{i\alpha\alpha'} = \sum_\beta^{G+I} \gamma_{\alpha\alpha',\beta} C_{i\beta}, \tag{18a}$$

$$\gamma_{\alpha\alpha',\beta} = \sum_i c_{\beta i} D_{i\alpha\alpha'}. \tag{18b}$$

Starting from this expansion, it is natural to decompose $D_{i\alpha\alpha'}$ into a G displacement $D^G_{i\alpha\alpha'}$ and an I displacement part $D^I_{i\alpha\alpha'}$ according to

$$D^Y_{i\alpha\alpha'} = \sum_\beta^Y \gamma_{\alpha\alpha',\beta} C_{i\beta}, \tag{19}$$

where $Y = \{G, I\}$. With this decomposition, Eq. (16b) can be rewritten as

$$d_{\alpha ik} = \sum_{\alpha'}^G (g_G^{-1})_{\alpha\alpha'} \left[\sum_\beta^G (c_{\beta i} D^I_{k\alpha'\beta} + c_{\beta k} D^I_{i\alpha'\beta}) - \sum_{\beta\beta'}^G \Gamma_{\beta\beta',\alpha'} c_{\beta i} c_{\beta' k} \right]. \tag{20}$$

The terms containing $D^I_{k\alpha'\beta}$ in Eq. (20) refer to force-constant contributions that mix G and I displacements, thus describing the impact of the interfragment dispersion forces on intrafragment vibrations. Given that the intrafragment dispersion forces have been neglected, it is not justified to incorporate these terms, and we will omit them in the following. This leads to

$$K_{ik} = \sum_{\beta\beta'}^G \bar{K}^{\mathrm{eff}}_{\beta\beta'} c_{\beta i} c_{\beta' k}, \tag{21a}$$

$$\bar{K}^{\mathrm{eff}}_{\beta\beta'} = \bar{K}_{\beta\beta'} - \sum_{\alpha\alpha'}^G (g_G^{-1})_{\alpha\alpha'} \Gamma_{\beta\beta',\alpha'} \bar{F}_\alpha. \tag{21b}$$

If the $\bar{F}_\alpha$ and $\bar{K}_{\alpha\beta}$ are known for a complete set of G displacements, one can use Eqs. (9a), (9b), (16a), (20), (21a), and (21b) to determine the corresponding F_i and K_{ik}.

Fore practical calculations, Eqs. (21a) and (21b), have to be worked out for a specific set of global displacements. We choose a set of displacements consisting of (i) a rotation of

fragment A by an angle $\boldsymbol{\varphi}$, (ii) a translation of the fragments against each other by a vector $\boldsymbol{\tau}$, performed in a way that the center of the molecule remains unchanged, (iii) a rotation of the whole molecule around an angle $\boldsymbol{\Phi}$, and (iv) a translation of the whole molecule by a vector $\mathbf{T}$. The displacements are to be performed in the order specified. Since each of the displacements (i)–(iv) is characterized by a (translation or rotation) vector, the set (i)—(iv) contains totally 12 independent displacements, which agrees with the total number of independent rigid displacements for fragments A and B. This choice of the displacements has the advantage that the six displacements in (iii) and (iv) describe rigid movements of the system as a whole, i.e., we need to calculate the energy gradients only for the six displacements in (i) and (ii), which describe movements of the fragments against each other. Up to second order, the atomic displacements expressed in Cartesian coordinates x_I, $I=1,\ldots,N$, have the form

$$x_I = \boldsymbol{\varphi} \times \mathbf{R}_{IA} + \tfrac{1}{2}\boldsymbol{\varphi} \times (\boldsymbol{\varphi} \times \mathbf{R}_{IA}) + \boldsymbol{\Phi} \times \mathbf{R}_I + \boldsymbol{\Phi} \times (\boldsymbol{\varphi} \times \mathbf{R}_I) + \tfrac{1}{2}\boldsymbol{\Phi} \times (\boldsymbol{\Phi} \times \mathbf{R}_I) + f_A \boldsymbol{\tau} + f_A \boldsymbol{\Phi} \times \boldsymbol{\tau} + \mathbf{T} \quad \text{for } I \in A, \tag{22a}$$

$$x_I = \boldsymbol{\Phi} \times \mathbf{R}_I + \boldsymbol{\Phi} \times (\boldsymbol{\varphi} \times \mathbf{R}_I) + \tfrac{1}{2}\boldsymbol{\Phi} \times (\boldsymbol{\Phi} \times \mathbf{R}_I) + f_B \boldsymbol{\tau} + f_B \boldsymbol{\Phi} \times \boldsymbol{\tau} + \mathbf{T} \quad \text{for } I \in B, \tag{22b}$$

$$f_A = \frac{N_B}{N}, \tag{22c}$$

$$f_B = -\frac{N_A}{N}. \tag{22d}$$

N_A and N_B are the numbers of nuclei in A and B. From Eq. (6), one finds the coefficients C as follows (we write the indices in parentheses rather than as subscripts to avoid double indices):

$$C(Ip,\varphi_q) = \sum_r \varepsilon_{pqr} R_{IA,r} \quad \text{for } I \in A, \tag{23a}$$

$$C(Ip,\varphi_q) = 0 \quad \text{for } I \in B, \tag{23b}$$

$$C(Ip,\Phi_q) = \sum_r \varepsilon_{pqr} R_{I,r}, \tag{23c}$$

$$C(Ip,\tau_q) = \delta_{pq} f_X, \tag{23d}$$

$$C(Ip,T_q) = \delta_{pq}. \tag{23e}$$

Here, $X=A,B$, indices p, q, and r denote Cartesian coordinates, and ε_{pqr} is the fully antisymmetric unit tensor of rank 3, i.e., $\varepsilon_{123}=1$, and $\varepsilon_{qpr}=\varepsilon_{rqp}=\varepsilon_{prq}=-\varepsilon_{pqr}$ for all p, q, and r. The metric tensor has the form

$$g(\varphi_p,\varphi_q) = \Theta_{A,pq}, \tag{24a}$$

$$g(\Phi_p,\varphi_q) = \Theta_{A,pq}, \tag{24b}$$

$$g(\Phi_p,\Phi_q) = \Theta_{pq}, \tag{24c}$$

$$g(\Phi_p,\tau_q) = \frac{N_A N_B}{N} \sum_r \varepsilon_{pqr} R_{AB,r}, \tag{24d}$$

$$g(\tau_p,\tau_q) = \delta_{pq} \frac{N_A N_B}{N}, \tag{24e}$$

$$g(T_p,T_q) = \delta_{pq}, \tag{24f}$$

where

$$\Theta_{A,pq} = \sum_I^A (R_{IA}^2 \delta_{pq} - R_{IA,p} R_{IA,q}), \tag{25a}$$

$$\Theta_{pq} = \sum_I^{A+B} (R_I^2 \delta_{pq} - R_{I,p} R_{I,q}) \tag{25b}$$

are fictitious tensors of inertia for the case that all nuclear masses are equal to 1. All other elements of the metric tensor are zero. The nonzero Christoffel symbols are

$$\Gamma(\varphi_q\varphi_r,\varphi_p) = \frac{1}{2}\sum_s (\varepsilon_{prs}\Theta_{A,qs} + \varepsilon_{pqs}\Theta_{A,rs}), \tag{26a}$$

$$\Gamma(\varphi_q\varphi_r,\Phi_p) = \Gamma(\varphi_q\varphi_r,\varphi_p), \tag{26b}$$

$$\Gamma(\Phi_q\Phi_r,\varphi_p) = \Gamma(\varphi_q\varphi_r,\varphi_p), \tag{26c}$$

$$\Gamma(\Phi_q\varphi_r,\varphi_p) = -\sum_s \varepsilon_{pqs}\Theta_{A,rs} + \frac{1}{2}\varepsilon_{pqr}\,\mathrm{Tr}\,\underline{\underline{\Theta}}_A, \tag{26d}$$

$$\Gamma(\Phi_q\varphi_r,\Phi_p) = \Gamma(\Phi_q\varphi_r,\varphi_p), \tag{26e}$$

$$\Gamma(\Phi_q\Phi_r,\Phi_p) = \frac{1}{2}\sum_s (\varepsilon_{prs}\Theta_{qs} + \varepsilon_{pqs}\Theta_{rs}), \tag{26f}$$

$$\Gamma(\Phi_q\Phi_r,\tau_p) = \frac{N_A N_B}{N}\left[\frac{1}{2}(\delta_{pr}R_{AB,q} + \delta_{pq}R_{AB,r}) - \delta_{qr}R_{AB,p}\right], \tag{26g}$$

$$\Gamma(\Phi_q\tau_r,\tau_p) = \varepsilon_{pqr}. \tag{26h}$$

Finally, we give the expressions for the $\bar{F}_\alpha$ and $\bar{K}_{\alpha\alpha'}$ elements required. Following Eq. (5), they can be written in the form

$$\begin{Bmatrix} \bar{F}_\alpha \\ \bar{K}_{\alpha\alpha'} \end{Bmatrix} = \frac{1}{2}\int_{V_A} d^3r_1 \int_{V_B} d^3r_2 W[\rho_A(\mathbf{r}_1), \nabla\rho_A(\mathbf{r}_1), \rho_B(\mathbf{r}_2), \nabla\rho_B(\mathbf{r}_2)] \begin{Bmatrix} \psi_\alpha(\mathbf{r}_1,\mathbf{r}_2) \\ \psi_{\alpha\alpha'}(\mathbf{r}_1,\mathbf{r}_2) \end{Bmatrix}. \tag{27}$$

Here, the ψ_α and $\psi_{\alpha\alpha'}$ are given by the expressions

$$\psi(\varphi_p) = (\mathbf{r}_{1A} \times \mathbf{r}_{12})_p \psi^\bullet, \tag{28a}$$

$$\psi(\tau_p) = r_{12,p}\psi^\bullet, \tag{28b}$$

$$\psi(\varphi_p,\varphi_q) = (\mathbf{r}_{1A}\times\mathbf{r}_{12})_p(\mathbf{r}_{2A}\times\mathbf{r}_{12})_q\psi^{\bullet\bullet} + \left[\frac{1}{2}(r_{1A,p}\mathbf{r}_{2A,q}+r_{1A,q}\mathbf{r}_{2A,p}) - \delta_{pq}\mathbf{r}_{1A}\mathbf{r}_{2A}\right]\psi^{\bullet}, \tag{28c}$$

$$\psi(\varphi_p,\tau_q) = (\mathbf{r}_{1A}\times\mathbf{r}_{12})_p r_{12,q}\psi^{\bullet\bullet} + \sum_r \varepsilon_{pqr}r_{1A,r}\psi^{\bullet}, \tag{28d}$$

$$\psi(\tau_p,\tau_q) = r_{12,p}r_{12,q}\psi^{\bullet\bullet} + \delta_{pq}\psi^{\bullet}, \tag{28e}$$

where $\mathbf{r}_{12}=\mathbf{r}_1-\mathbf{r}_2$, $\mathbf{r}_{1A}=\mathbf{r}-\mathbf{R}_A$, and $\mathbf{r}_{1B}=\mathbf{r}-\mathbf{R}_B$ and

$$\psi^{\bullet} = \left[\frac{1}{r}\frac{d\psi}{dr}\right]_{r=r_{12}}, \tag{29a}$$

$$\psi^{\bullet\bullet} = \frac{1}{r}\frac{d}{dr}\left[\frac{1}{r}\frac{d\psi}{dr}\right]_{r=r_{12}}. \tag{29b}$$

The explicit expression for $\psi^{\bullet}$ and $\psi^{\bullet\bullet}$ depends on the form of the damping functions h chosen in Eq. (3). In the present work, we use[50]

$$h(r) = \exp-\left(\frac{a}{r}\right)^6 \tag{30}$$

(see Sec. II B for the choice of the parameter a), which implies

$$\psi^{\bullet} = \frac{6}{r_{12}^8}(-1+Q)e^{-Q}, \tag{31a}$$

$$\psi^{\bullet\bullet} = \frac{6}{r_{12}^{10}}[7+(-14+6Q)Q]e^{-Q}, \tag{31b}$$

$$Q = \left(\frac{a}{r_{12}}\right)^6, \tag{31c}$$

where r_{12} is the distance between two electrons, one in fragment A and one in fragment B. Equations (10a), (21a), (21b), (23a)–(23e), (24a)–(24f), (25a), (25b), (26a)–(26h), (28a)–(28e), (30), and (31a)–(31c) form the set of working equations.

If one or both of the fragments are monatomic or linear, some of the $C_{i\alpha}$ ($\alpha\in G$) are linearly dependent or identically zero, and the metric tensor becomes singular. To handle this case properly, the tensor g_G^{-1} has to be determined in the sense of the generalized inverse introduced by Peng *et al.*[106] In the general case, where g is regular, the generalized inverse is identical to the usual one. If g is singular, the generalized inverse will project out contributions that correspond to the linearly dependent or vanishing $C_{i\alpha}$ vectors.

The formalism presented above is straightforward to generalize to the case of weighted Cartesian coordinates,

$$X_{Ip} = w_I x_{Ip}, \tag{32}$$

where w_I are constant weight factors.

There may be two reasons to use weighted coordinates:

(i) If the algorithm is to be used in connection with molecular dynamics or reaction-path following investigations, mass-weighted coordinates have to be applied, i.e.,

$$w_I = \sqrt{M_I}, \tag{33}$$

where M_I is the mass of nucleus I.

(ii) For extended fragments, the coordinates should be weighted in a way that the centers $\mathbf{R}_A$ and $\mathbf{R}_B$ are moved closer to the dispersion interaction region. Otherwise, the assumption that I displacements do not contribute to the dispersion force may be questionable. In this case, the w_I may be chosen in a way that atoms in the dispersion region obtain a larger weight and atoms farther away a smaller one. A simple choice is (we assume $I\in X$)

$$w_I = \sum_{K\notin X}\psi(|\mathbf{R}_I-\mathbf{R}_K|). \tag{34}$$

To introduce mass-weighted coordinates, one simply has to reformulate Eq. (6) in terms of the X_i, which implies that all $C_{i\alpha}$ and $D_{i\alpha\beta}$ will be multiplied by the corresponding weight factors w_I. Then, the procedure is continued with the modified $C_{i\alpha}$ and $D_{i\alpha\beta}$, providing elements F_i and K_{ik} in terms of the X_i.

B. Implementation of quasi-SCF-DC-DFT

We implemented the LR-HF and the SR-PBE exchange functionals, i.e., we split the Coulomb potential $v_{\mathrm{Coul}}(r)=1/r$ according to

$$\frac{1}{r} = \frac{1-\mathrm{erf}(\mu r)}{r} + \frac{\mathrm{erf}(\mu r)}{r}, \tag{35}$$

where the first term describes the SR part and is treated by DFT whereas the second term on the right hand side accounts for the LR part of the Coulomb interaction and is treated exactly. The parameter μ controls the separation between SR and LR parts. Following Hirao and co-workers,[50–52] we chose $\mu=0.33$.

In addition, we programed the OP SR-correlation functional and the ALL LR-correlation functional, including the formalism described in Sec. II B, in the COLOGNE08 quantum chemistry program package.[107] For the OP functional, we followed the original work by Hirao and co-workers;[50,51] for the SR-PBE functional, we used the parametrization suggested by Toulouse *et al.*[104] The LR-HF functional was implemented based on the algorithm suggested by Panas[85] and by Adamson *et al.*[87] For all exchange and correlation terms, first and second analytic gradients were provided.

The implementation of the ALL functional[49] required a number of modifications in order to ensure numerical stability. The original expression for the kernel W in Eq. (2) reads

$$W[\rho_A(\mathbf{r}_1),\nabla\rho_A(\mathbf{r}_1),\rho_B(\mathbf{r}_2),\nabla\rho_B(\mathbf{r}_2)] = \frac{3}{2(4\pi)^{3/2}}\frac{\rho_A^{1/2}(\mathbf{r}_1)\rho_B^{1/2}(\mathbf{r}_2)}{\rho_A^{1/2}(\mathbf{r}_1)+\rho_B^{1/2}(\mathbf{r}_2)} \times\Theta\left(1-\frac{1}{3(9\pi)^{1/6}}\frac{|\nabla\rho_A(\mathbf{r}_1)|}{\rho_A(\mathbf{r}_1)^{7/6}}\right) \times\Theta\left(1-\frac{1}{3(9\pi)^{1/6}}\frac{|\nabla\rho_B(\mathbf{r}_2)|}{\rho_B(\mathbf{r}_2)^{7/6}}\right), \quad (36)$$

where $\Theta(x)$ is the Heaviside step function. Test calculations indicated that the sharp cutoff provided by the Heaviside function gives rise to numerical noise, in particular, when rotations of fragments are considered. Therefore, we replaced the Θ function in Eq. (36) by a Fermi function $\Theta_\varepsilon(x)$ according to

$$\Theta_\varepsilon(x) = \frac{1}{e^{\varepsilon x}+1}. \quad (37)$$

Similarly, the restriction of the integral in Eq. (36) to the volumes V_A and V_B may result in numerical noise. Therefore, we replace the abrupt cutoff at the boundaries of V_A and V_B by a smooth cutoff according to

$$\int_{V_A} d^3r_1\int_{V_B} d^3r_2 \rightarrow \int d^3r_1\int d^3r_2\Theta_A(\mathbf{r}_1)\Theta_B(\mathbf{r}_2), \quad (38)$$

where the cutoff functions are chosen according to

$$\Theta_A(\mathbf{r}) = \Theta_\varepsilon\left[\frac{\min_{I\in A}|\mathbf{r}-\mathbf{R}_I| - \min_{K\in B}|\mathbf{r}-\mathbf{R}_K|}{s_0}\right], \quad (39a)$$

$$\Theta_B(\mathbf{r}) = 1-\Theta_A(\mathbf{r}), \quad (39b)$$

where $s_0=a_0/20$ was used (a_0 is the Bohr radius).

For the factor a in $h(r)$ from Eq. (30), we follow the scheme given by Hirao and co-workers[50,51] and define a on a per-atom-pair basis. This implies that we decompose the integral in Eq. (36) in a sum of atom-pair contributions:

$$h(r_{12}) = \sum_{I\in A}\sum_{K\in B} w_I(\mathbf{r}_1)w_K(\mathbf{r}_2)h_{IK}(r_{12}), \quad (40a)$$

$$h_{IK}(r_{12}) = \exp\left[-\left(\frac{a_{IK}}{r}\right)^6\right], \quad (40b)$$

$$a_{IK} = a_0 + a_1(r_{\mathrm{vdW},I} + r_{\mathrm{vdW},K}). \quad (40c)$$

As suitable w_I and w_K atomic weights, we use Stratmann–Scuseria weights.[108] Symbol $r_{\mathrm{vdW},I}$ denotes the vdW radius of atom I, which are determined via the $0.001a_0^{-3}$ electron density contour line from atomic ROHF (Restricted Open-shell Hartree-Fock) calculations.[109] The coefficients $a_0=1.8949$ and $a_1=0.429$ are taken from the work of Kamiya *et al.*[50] Technically, the contribution for each pair I, K in Eq. (40) will be calculated separately with a suitable pair of atomic integration grids centered around $\mathbf{R}_I$ and $\mathbf{R}_K$, respectively.

The densities ρ_A and ρ_B are determined by projecting the molecular orbitals (MOs) of the molecule on the set of atomic orbitals belonging to A or B, respectively. For consistence, the atomic weights w_I have to be determined separately within each fragment, i.e., with the normalization

$$\sum_{I\in X} w_I(\mathbf{r}) = 1. \quad (41)$$

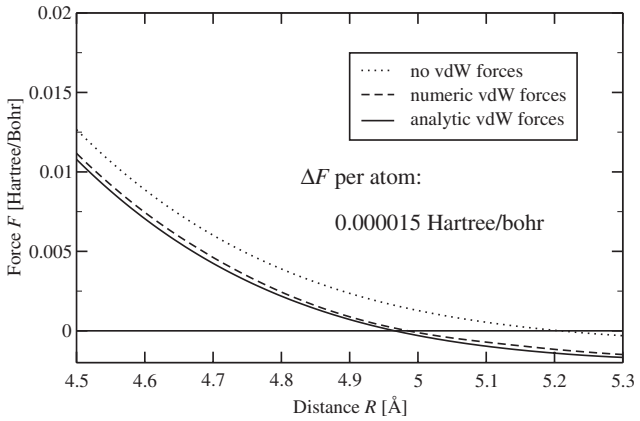

FIG. 1. Forces between the benzene monomers for the T-AoA form of the benzene dimer (see Fig. 2) in dependence of the interfragment distance R as calculated with vdW forces excluded (dotted lines), calculated numerically (dashed line), and calculated analytically (solid line). For the definition of R, see Fig. 2. Calculations done with the SR-PBE+LR-HF+OP+ALL functional; for details of the calculation, see Sec. II B. Numeric forces calculated with a step width for R of 0.02 Å.

For the purpose of verifying that assumption (a) in Sec. II A is justified we performed a scan with respect to the interfragment distance R for the T-shaped benzene dimer with atom-over-atom arrangement (T-AoA) and compared analytically and numerically calculated interfragment forces in dependence on R. In this scan, the geometries of the two fragments were kept rigid to the equilibrium geometry of the benzene monomer, and the step width for R was chosen as 0.02 Å. Figure 1 shows the total interfragment forces for this case calculated with analytical and numerical dispersion forces and, for reference, the interfragment force with the dispersion term omitted. One finds that the analytically calculated forces are about 1.8×10^{-4} a.u. more attractive in the region around the equilibrium geometry. As the fragments get closer to each other, the charge clouds avoid each other due to exchange repulsion, which reduces the dispersion interaction and thus the attractive dispersion force. This effect is neglected for the analytical dispersion energy gradients, which accounts for the overestimation of forces. The deviation of 1.8×10^{-4} a.u. corresponds to a deviation of about 1.5×10^{-5} a.u. per atom, which is below the convergence threshold [about $(3-5)\times10^{-4}$ a.u.] in most quantum chemistry packages. The exaggeration of the attractive dispersion forces results in a decrease in the equilibrium interfragment distance R_e. It should be noted that the R_e scan with analytical forces yields $R_e=4.970$ Å for the T-AoA complex, which differs by 0.006 Å from the value found in the geometry optimization (Table II). This difference is caused by the relaxation of the benzene monomers incorporated in the geometry optimization.

We found that a SR-PBE+LR-HF+OP+ALL calculation typically requires about 10%–20% more central processing unit (CPU) time than a corresponding SR-PBE+LR-HF

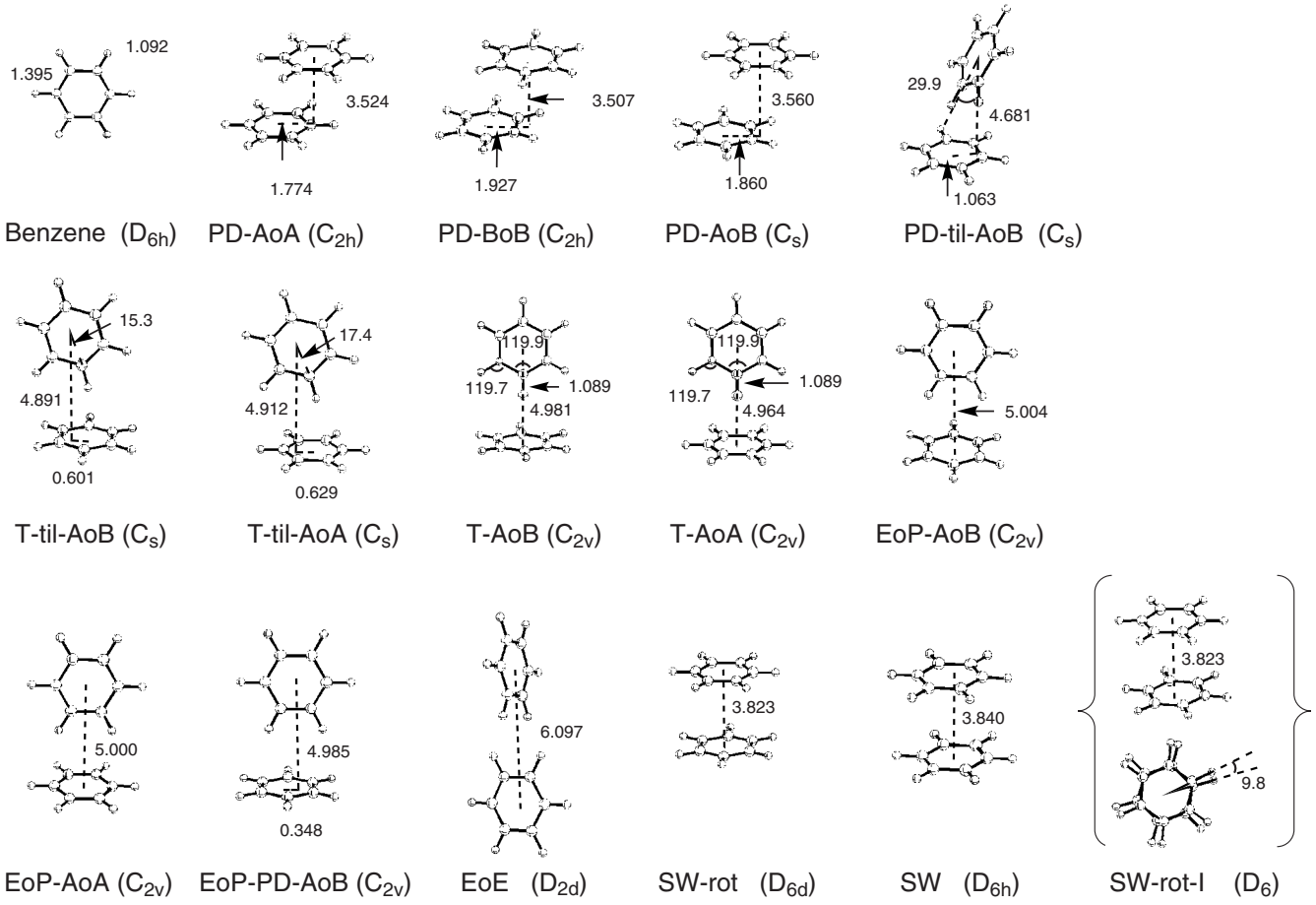

FIG. 2. Ball and stick representations of the 16 benzene dimer forms calculated in this work. For each form, the appropriate notation and the symmetry are given. Dashed lines indicate distances between geometrical centers of the monomers and possible sideward shifts. Some geometrical parameters are given that are not included in Table II. Distances in Å and angles in degrees.

+OP calculation without DC term. This is in line with the findings by Thonhauser *et al.*[55] that a non-SCF calculation of the DC term implies only a minor increase in CPU time.

All calculations were performed with the COLOGNE08 program package.[107] The aug-cc-pVDZ basis set of Dunning, Jr.[110] was used for C atoms and its cc-pVDZ equivalent set for H atoms. In this way, the diffuse tails of the π MO of benzene are appropriately described by a set of diffuse *sp* functions whereas the densities at the H atoms are more compact and do not require diffuse functions. Counterpoise corrections[111] were applied to all calculated dimer binding energies to eliminate basis-set superposition errors (BSSEs). Energy gradients and second derivatives were calculated analytically.

III. APPLICATION TO THE BENZENE DIMER

The QSCF-DC-DFT method described in Sec. II has been applied to the benzene dimer employing the SR-PBE +LR-HF+OP+ALL XC functional. A total of 16 stationary points have been found on the PES of the benzene dimer, 10 of which were described previously in the literature by utilizing SAPT(DFT) theory[33] and more recently by using PBE(CCSD(T)) (error corrected DFT).[47] The 16 forms are shown in Fig. 2 where the following notation has been used to distinguish between the individual complex forms: The abbreviations PD, T, and SW denote the parallel-displaced sandwich, the T, and the sandwich forms. These are further characterized by indicating whether a H–C···C–H fragment of the upper benzene is exactly located over a H–C···C–H fragment of the lower benzene (AoA) or bisects two CC bonds of the lower benzene [atom-over-bond (AoB) arrangement]. It is also possible that the two benzene rings are eclipsed [bond-over-bond (BoB) arrangement], which corresponds to the SW form with D_{6h} symmetry whereas the D_{6d}-symmetrical SW form represents an AoB arrangement of the benzene rings. Hence, the PB-AoB form results from a parallel displacement of the SW form by an AoB shift. If the rings are tilted (til) with regard to each other, one will get the PD-til-AoB form (Fig. 2).

In the same way, one can distinguish between the four different T forms. EoP and EoE denote edge-over-plane and edge-over-edge forms where the former can have AoA, AoB, or PD-AoB arrangements (Fig. 2). Rotational intermediate (SW-rot-I) and rotational forms of the SW structure (SW-rot) are not further characterized with regard to AoA or AoB arrangement. With the abbreviations introduced here it is possible to describe the different rearrangements of the benzene dimer investigated in this work.

Energies and geometries of the 16 forms shown in Fig. 2 are listed in Tables I and II. The geometrical parameters shown in Fig. 2 complement those of Table II and help (al-

TABLE I. Energies, thermochemistry, and characterization of calculated stationary points for the different forms of the benzene dimer. (Calculations were done with the SR-PBE+LR-HF+OP+ALL functional and the aug-cc-pVDZ basis for C atoms and cc-pVDZ basis set for H atoms of Dunning (Ref. 110). See Fig. 2 for the structure and geometry of the dimers. Monomer: $E=-231.994\ 169\ 8$ a.u. and ZPE=63.02 kcal mol^{-1}. All energies are in kcal mol^{-1} and wave numbers in cm^{-1}. The notation of the various forms is described in the text and uses the following abbreviations: PD, parallel displaced; T, T form; SW, sandwich form; AoA, atom over atom; AoB, atom over bond; BoB, bond over bond; til, tilted; rot, rotated; I, intermediate. M, SP1, SP2, and SP3 denote minimum, first order, second order, and third order saddle points.)

Notation											$\bar{\nu}_{\text{imag}}$	
Ref. 33	This work	Sym	D_e [a]	$E_{\text{C,vdW}}$	D_e [b]	BSSE	D_e [c]	ΔZPE	D_0	Type	Value	IRREP
M1	PD-AoA	C_{2h}	0.26	−3.48	−3.22	0.54	−2.68	0.28	−2.40	M		A_u
⋯	PD-BoB	C_{2h}	0.25	−3.37	−3.12	0.55	−2.57	0.26	−2.31	SP2	21.8i	A_u
											9.1i	B_g
S2	PD-AoB	C_s	0.14	−3.34	−3.20	0.52	−2.68	0.25	−2.43	SP1	10.3i	A''
S4	PD-til-AoB	C_s	−0.68	−2.56	−3.24	0.52	−2.72	0.41	−2.31	SP1	25.7i	A''
M2	T-til-AoB	C_s	−0.86	−2.50	−3.36	0.53	−2.84	0.44	−2.40	M		
S1	T-til-AoA	C_s	−0.92	−2.44	−3.36	0.52	−2.83	0.43	−2.40	SP1	13.5i	A''
S3	T-AoB	C_{2v}	−0.88	−2.42	−3.30	0.50	−2.80	0.39	−2.41	SP1	27.9i	B_2
⋯	T-AoA	C_{2v}	−0.87	−2.42	−3.29	0.51	−2.77	0.41	−2.37	SP2	28.9i	B_2
											11.1i	A_2
S5	EoP-AoB	C_{2v}	−0.55	−2.34	−2.88	0.43	−2.45	0.31	−2.14	SP1	40.9i	A_2
⋯	EoP-AoA	C_{2v}	−0.57	−2.35	−2.92	0.47	−2.45	0.36	−2.09	SP1	41.3i	B_2
⋯	EoP-PD-AoB	C_s	−0.57	−2.37	−2.95	0.45	−2.50	0.33	−2.17	SP1	37.0i	A'
M3	EoE	D_{2d}	−0.33	−2.05	−2.38	0.53	−1.85	0.37	−1.48	SP1	15.1i	E
S7	SW	D_{6d}	1.09	−3.36	−2.27	0.46	−1.82	0.20	−1.62	SP3	43.0i	E_5
											17.8i	B_1
S8	SW-rot	D_{6h}	1.09	−3.37	−2.28	0.46	−1.82	0.20	−1.62	SP3	40.4i	E_{1g}
											11.6i	A_{1u}
⋯	SW-rot-I	D_6	1.06	−3.42	−2.36	0.49	−1.87	0.24	−1.63	SP2	44.2i	E_1

[a]Without $E_{\text{C,vdW}}$.
[b]With $E_{\text{C,vdW}}$.
[c]With $E_{\text{C,vdW}}$ and counterpoise corrections.

though redundant) compare calculated geometries that are not following the coordinate system used in Table II: R, distance between the geometrical centers of the two rings, and θ_1 and θ_2, tilting angles of the benzene rings relative to the connection line between the geometrical centers. For the latter values, 0°, 180°, and 90° arrangements are not explicitly listed. Table II contains also SAPT(DFT) (Ref. 33) and PBE(CCSD(T)) geometries (Ref. 47) for comparison. A comparison of calculated binding energies with those obtained from high level *ab initio*[33,34,40,47] and other DFT calculations[33,47,56,80] is given in Table III.

In agreement with the majority of all other investigations

TABLE II. Comparison of QSCF-DC-DFT with SAPT(DFT) and PBE(CCSD(T)) geometries for the benzene dimer.[a]

Notation			This work			SAPT(DFT)			PBE(CCSD(T))		
Ref. 33	This work	Sym	R	θ_1	θ_2	R	θ_1	θ_2	R	θ_1	θ_2
M1	PD-AoA	C_{2h}	3.945	63.9	63.9	3.962	61.0	61.0	3.89	63.9	63.9
⋯	PD-BoB	C_{2h}	4.001	61.2	61.2						
S2	PD-AoB	C_s	4.014	61.8	63.1	3.973	63.2	63.2	3.89	63.8	63.8
S4	PD-til-AoB	C_s	4.798	77.2	17.1	4.453	66.9	36.0	4.73	75.3	21.6
M2	T-til-AoB	C_s	4.931	97.0	8.3	4.954	99.6	11.7	4.93	100.0	13.5
S1	T-til-AoA	C_s	4.952	97.3	10.1	4.960	98.6	10.9	4.94	99.6	13.3
S3	T-AoB	C_{2v}	4.981			4.982			5.01		
⋯	T-AoA	C_{2v}	4.964								
S5	EoP-AoB	C_{2v}	5.004			5.026			5.00		
⋯	EoP-AoA	C_{2v}	5.000								
⋯	EoP-PD-AoB	C_s	4.985	94.0	4.3						
M3	EoE	D_{2d}	6.097			6.104			6.09		
S7	SW	D_{6d}	3.823			3.793			3.87		
S8	SW-rot	D_{6h}	3.840			3.807			3.87		
⋯	SW-rot-I	D_6	3.823	9.8[b]							

[a]R (in Å) and θ_1 and θ_2 (in degree) are defined in the text. This work: SR-PBE+LR-HF+OP+ALL functional and the aug-cc-pVDZ basis for C atoms and cc-pVDZ basis set for H atoms of Dunning (Ref. 110) SAPT(DFT): Ref. 33. PBE(CCSD(T)): Ref. 47. Distances in Å and angles in degrees.
[b]Mutual torsion of the two monomers.

TABLE III. Comparison of dissociation energies D_e obtained for the benzene dimer with different methods. (D_e values in kcal/mol. For the notation of stationary points see Fig. 2 and text. The characterizations as M2, M1, T, and S8 are taken from Ref. 33.)

Stationary point	T-til-AoB	PD-AoA	T-AoB	SW	Ref.
	Min	Min	SP1	SP3	This work
Method[a]	M2	M1	T	S8	33
QSCF-DC-DFT	−2.84	−2.68	−2.80	−1.82	This work
CCSD(T)/CBS		−2.72	−2.68	−1.71	34
CCSD(T)/CBS	−2.82	−2.73	−2.70	−1.71	47
QCISD(T)/CBS		−2.66	−2.68	−1.65	40
CCSDT/AVTZ+b	−2.80	−2.70	−2.68	−1.68	33
SAPT(DFT)AVTZ+b	−2.77	−2.74	−2.66	−1.85	33
PBE/CCSD(T)	−2.72	−2.68	−2.57	−1.70	47
vdW-DFT		−2.80	−2.28	−2.37	56
DFT-D/TZV2P		−2.75	−2.99	−1.77	80

[a]CCSD(T)/CBS (Ref. 34): CCSD(T)/AVTZ*, basis-set effects estimated at the SCS-MP2 level using AVQZ* and AV5Z* extrapolations; CCSD(T)/CBS (Ref. 47: CCSD(T)/AVDZ, CBS expansion calculated at the SCS-MP2 level using the AVTZ and AVQZ basis sets; SAPT(DFT)AVTZ+b: PBE0 XC functional used; vdW-DFT: nonlocal density-functional calculations using the plane-wave basis set (energy cutoff of 50 Ry); DFT-D/TZV2P: using a reparametrized B97-D-functional.

we find that the T-til-AoB benzene dimer is located at the global minimum of the PES, possessing a dissociation energy D_e of 2.84 kcal/mol (Table I). This form is slightly stable at the KS level of theory (−0.86 kcal/mol) but gains another −2.50 kcal/mol by the dispersion term, which is corrected by 0.53 kcal/mol for BSSE. The ZPE correction leads to another reduction (0.44 kcal/mol) so that the final D_0 value is just 2.40 kcal/mol, in excellent agreement with the accepted experimental D_0 value of 2.4 ± 0.4 kcal/mol.[16] A much lower experimental value of 1.6 ± 0.2 kcal/mol (Ref. 17) is in conflict with all reliable quantum chemical calculations and has to be discarded.

In the minimum form T-til-AoB, the upper benzene ring is tilted by 17.4° and shifted by 0.63 Å (Fig. 2) so that dispersion forces are slightly increased relative to those of the C_{2v}-symmetrical T forms (Table I). Parameter R is 4.93 Å (Table II) close to the SAPT(DFT) value[33] and identical to the corresponding PBE(CCSD(T)) value[47] (Table II). Changes in the monomer geometries (which are routinely obtained by QSCF-DC-DFT at no extra cost) are in the range of 0.001 Å and 0.1°.

A second minimum was found for the PD-AoA form that possesses a D_e value of 2.68 kcal/mol (Table I), a plane to plane distance of 3.52, and a sideward shift of 1.77 Å (Fig. 2). The distance R calculated by QSCF-DC-DFT (3.95 Å) agrees with the SAPT(DFT) value of 3.96 Å (Ref. 33) but differs slightly from the 3.89 Å obtained at the PBE(CCSD(T)) level.[47] CCSD(T) values of R are close to 3.9 Å as cited in Ref. 33. The binding energy calculated (2.68 kcal/mol after a BSSE correction of 0.54 kcal/mol) is 0.04 kcal/mol larger than the best CCSD(T) result (2.72 kcal/mol,[34] Table III) obtained so far, which again suggests high accuracy of the QSCF-DC-DFT approach.

The ZPE correction of just 0.28 kcal/mol leads to a D_0 value of 2.40 kcal/mol identical to the T-til-AoB value, which would mean that the two forms effectively have the same binding energy D_0 [in line with the CCSD(T)/CBS values of Table III]. This result, however, has to be seen on the background that CCSD(T)/CBS may differ from the exact result by 0.05 kcal/mol due to missing quadruple effects [estimated D_0 of 2.30 kcal/mol (Ref. 97)], thus giving still some preference to the T-til-AoB form. In this connection we note that the QSCF-DC-DFT method used in this work has not been parametrized in any way, especially not for the description of the benzene dimer. Therefore, the method should perform for the two structures equally well.

In Table III two other forms that have been frequently investigated in the past because of their high symmetry (thus reducing calculational cost), the T-AoB and the SW form, are compared. QSCF-DC-DFT describes T-AoB as a SP1 with one imaginary frequency ($28i$ cm^{-1}, Table I) associated with a B_2 mode (rotation of one of the benzene rings) whereas the D_{6h}-symmetrical SW turns out to be a SP3. Lowering of the energy can be achieved by AoA or BoB E_{1g}-symmetrical shifts or third by an A_{1u}-symmetrical rotation of one of the benzene rings [see PES diagram in Fig. 3(b)]. SW is connected to another SP3 occupied by the D_{6d}-symmetrical SW-rot form of the same D_e (1.82 kcal/mol, Table I) but separated by a SP2 occupied by the D_6-symmetrical SW-rot-I form with $D_e = 1.87$ kcal/mol. In previous investigations SW-rot-I was not found because surface scans or numerical geometry optimizations make it difficult to locate lower symmetry forms. SW-rot-I is slightly stabilized by a balance between dispersion and electrostatic forces. Although this part of the PES of the benzene dimer is of limited relevance for the stability and dynamics of the complex, the frequent investigation of SW forms makes it a necessary benchmark test for any new method.

The data in Table III reveal that in the series T-til-AoB, PD-AoA, T-AoB, and SW with decreasing D_e values, QSCF-DC-DFT (2.84, 2.68, 2.80, and 1.82 kcal/mol, Tables I and III) overbinds slightly by 0.02, 0.04, 0.10, and 0.11 kcal/mol compared to the best CCSD(T)/CBS results listed in Table III [2.82, 2.72, 2.70, and 1.71 kcal/mol (Ref. 47)]. In the case of T-AoB, this has partly to do with a slight change in the monomer geometries (Fig. 2) but in general less with the

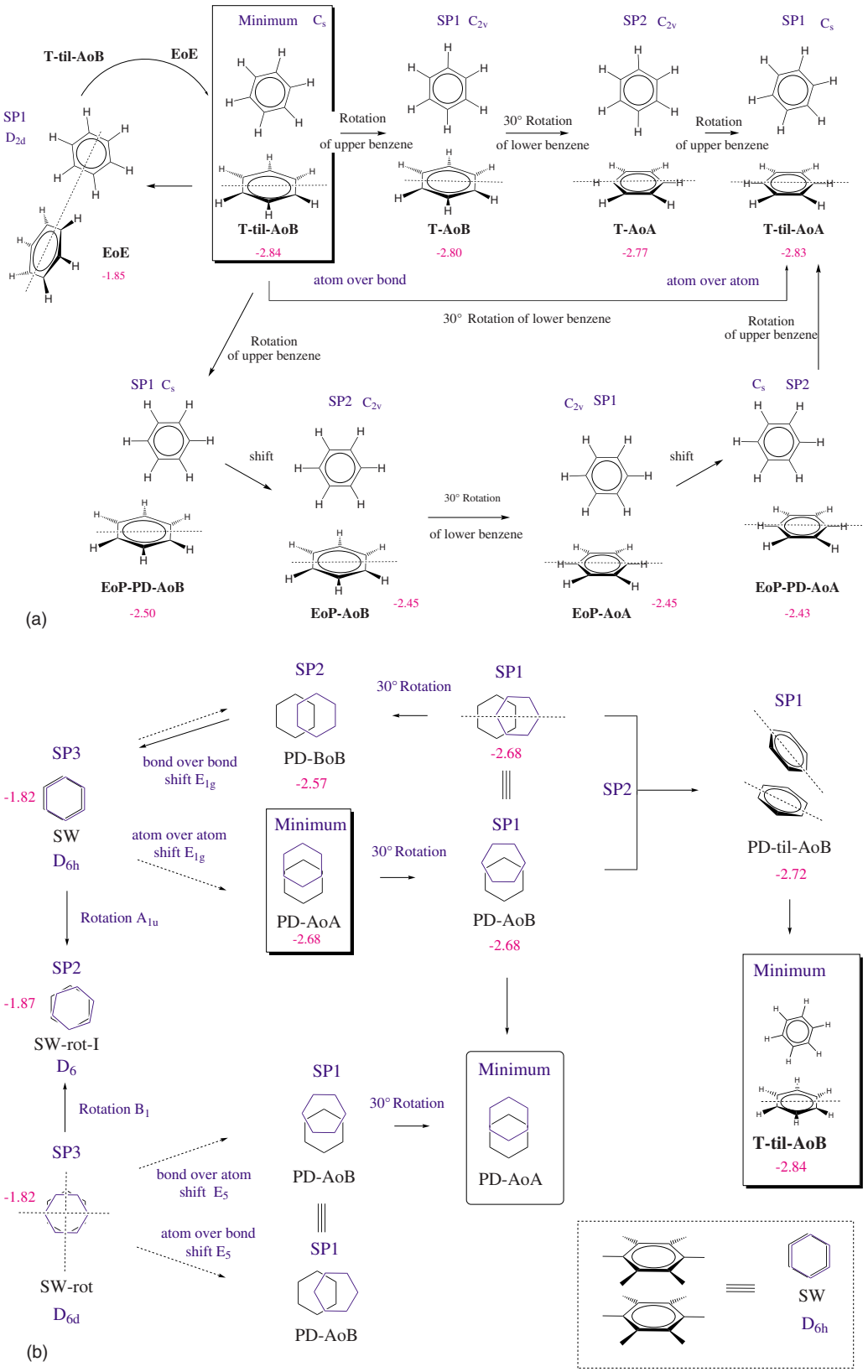

FIG. 3. (Color online) (a) Schematic description of the PES region hosting the PD forms. For reasons of simplification only the carbon rings are shown, the one on the top in blue in the online version, gray in the print version and the one at the bottom in black using apart from the two exceptions on the right side the top view. (b) Schematic description of the PES region hosting the T and EoP forms. The proper notation, symmetry, D_e values, and the character of the stationary point are given.

parameters R, θ_1, and θ_2, which nicely agree with the available CCSD(T), SAPT(DFT), and PBE(CCSD(T)) values (Table II).[33,47] With the present QSCF-DC-DFT calculations, a level of agreement between DC-DFT and the best CCSD(T) results has been reached that does not indicate whether the differences obtained result from incomplete optimization of the CCSD(T) geometries, frozen core approximations, the frozen geometry approximation for the mono-

mers in all previous calculations, the approximations with regard to the forces in the QSCF algorithm or any lack of higher order correlation effects in the methods used. In any case, we have obtained a substantial improvement for the description of the benzene dimer forms compared to previous vdW-DFT calculations of Puzder *et al.*[56] or Sato *et al.*[32] Clearly, we cannot produce identical CCSD(T)/CBS results as obtained with PBE(CCSD(T)) (Ref. 47) because such a method is parameterized for the purpose of reproducing CCSD(T)/CBS results. However, any parametrization will reach its limits when suitable reference data are missing, which is not the case for the method used in this work. For the benzene dimer PES, QSCF-DC-DFT performs equally well or even better than SAPT(DFT) (Ref. 33) or DFT-D,[80] although it excludes empirical parametrization (DFT-D) and stays within the realm of KS-DFT.

While working with QSCF-DC-DFT we found that in the situation of very flat PES intrarotational movements of a complex can lead to spurious imaginary frequencies (about $10i$ cm^{-1}), which, however, can be easily identified and eliminated.

A. Topology of the PES

In Fig. 3, those parts of the PES that have been explored with QSCF-DC-DFT are schematically shown. The SW forms correspond to small energy maxima in a reduced configuration space, which are surrounded by six minima of the PD-AoA type and six SP2 of the PD-BoB type. Rotation of one benzene molecule relative to the other via a SP1 occupied by PD-AoB is essentially free [D_e=2.68 kcal/mol, Fig. 3(a)].

The PD part of the PES is connected to the T part via a SP1 occupied by PD-til-AoB [S4 in Ref. 33, D_e =2.72 kcal/mol, Table I and Fig. 3(b)], which is likely to be connected to SP1 PD-AoB via a somewhat higher lying SP2 (not found in this work). We investigated three possible rearrangements of the minimum form T-til-AoB [Fig. 3(b)]: (a) a rotation of the lower benzene by two times 30° leading via the SP1 occupied by T-til-AoA back to T-til-AoB; (b) a combined rotation of the upper and lower benzene rings leading via T-AoB (SP1) and T-AoA (SP2) also to T-til-AoA; (c) a rotation of the upper benzene leads to the EoP forms that can rearrange via two SP1 and two SP2 also to T-til-AoA; (d) finally, the rearrangement into the EoE form [SP1, D_e =1.85 kcal/mol, Fig. 3(a)] and back into the T-til-AoB minimum.

The EoP forms are 0.3–0.4 kcal/mol higher in energy, whereas the EoE form is less stable than T-til-AoB by 1 kcal/mol. The EoE form was previously described as a M3 minimum[33] separated from the T-til-AoB minimum via a SP1 called S6.[33] Our calculations show that S6 does not exist on the QSCF-DC-DFT PES and that EoE is a SP1 rather than a minimum, in agreement with observations made by Bludsky *et al.*[47]

The PES is extremely flat in the range of the T forms and in that of the EoP forms [changes by 0.07 kcal/mol, Fig. 3(a)] and therefore any exploration of these parts of the PES with numerical or approximate methods is condemned to failure. Also, one has to consider whether a given method can consistently describe the various dimer forms and whether from a calculational and/or chemical point of view such an investigation is justified. We have investigated the PES to test accuracy and consistency of QSCF-DC-DFT on the background of similar studies carried out in the near past.[33,47] The chemical significance of this study becomes obvious when comparing calculated D_0 values (Table I). All stationary points in the PD and T parts of the PES host benzene dimer forms that have D_0 values within a range of just 0.12 kcal/mol (2.31–2.43 kcal/mol, Table I). Even at temperatures close to zero, the flatness of the PES leads to large-amplitude motions that make it difficult to specify which dimer form is dominating.

IV. CONCLUSIONS AND OUTLOOK

In the current work, QSCF-DC-DFT has been presented as an effective method for routine DFT calculations with dispersion incorporated and applied to the investigation of the benzene dimer PES. These investigations led to the following conclusions on QSCF-DC-DFT:

(a) The QSCF-DC-DFT algorithm integrates the ALL functional[49] completely into the framework of DFT. Geometry optimizations, frequency calculations, molecular dynamic simulations, and explorations of any multidimensional PES can be performed with standard techniques. The increase in computer time consumption compared to a standard KS-DFT calculation is small ($\leq$30%). The routine calculation of analytical energy derivatives makes it possible that the monomers in a vdW complex are reoptimized at no extra computational cost. Thus, geometry changes in the complex fragments caused, e.g., by steric or electrostatic forces can be detected during the optimization of the complex. Small geometrical changes in the monomers help identify the nature of their interactions. Larger changes in the monomer geometry can reveal deficiencies of the XC functional used as we found when balancing SR and LR parts of the DC-DFT XC functional.

(b) Replacing the step-function cutoff in the original ALL functional by a smoothed Fermi-function cutoff reduces the overbinding of vdW complexes observed by Hirao and co-workers.[50,51] There is no stringent reason that the cutoff in the ALL functional should be performed by a step function. Our results suggest that a smoothed cutoff gives a more appropriate description of the LR correlation than the sharp cutoff in the original ALL functional.

(c) The development of LR-correlation functionals is an active field with a distinctive potential for improvements. For instance, incorporating density gradients in the description of the electron correlation (as is done in the DRSLL functional[53,54]) gives a more detailed account of the electron structure inside the fragments. Likewise, the determination of the dielectric function of the electron system, which governs correlation effects, can be refined.[53,54] This kind of improvement will be of particular use for the treatment of extended

fragments and for the investigation of higher orders in the dispersion interaction (R^{-8} terms etc.)

The QSCF algorithm is not tied to the ALL functional. Thus, improvements in the available LR-correlation functionals will improve the accuracy and extend the applicability of the QSCF-DC-DFT approach.

Given these facts, we conclude that QSCF-DC-DFT is a promising method for the description of large molecules such as nanomaterials or biomolecules incorporation the investigation of geometry effects. To fully exploit the potential of QSCF-DC-DFT, the method should be extended and refined in several ways:

(1) *Technical refinement.* (i) The integration grids used for standard DFT integration are not optimally suited for the calculation of the double integrals in $E_{C,DC}$ because their resolution in the core region is unnecessarily high for this purpose. The double integrations in $E_{C,DC}$ should be done with purpose-designed grids. (ii) In large systems, atoms far away from each other make little or no contribution to the dispersion energy. Thus, screening strategies are required for an efficient treatment of large systems.
(2) For systems consisting of more than two fragments, the generalization of the QSCF-DC-DFT method is straightforward. In extension, the method provides a way to treat molecular crystals, whose components are bound mainly by dispersion attraction.
(3) As a by-product, the separation of global and intrafragment forces provides a counterpart to the SHAKE algorithm[112] used in classical molecular dynamics to suppress rapid intrafragment motions from the slower interfragment motions.
(4) Recently, we succeeded in reformulating ring puckering[113] in a way that allows an explicit separation between puckering and nonpuckering displacements.[114] With the algorithm presented in this work, it is possible to extract the force constants for the puckering displacements.

QSCF-DC-DFT has been applied to the benzene dimer, which is a benchmark problem for both highly correlated *ab initio* methods and dispersion-improved DFT methods. We have shown that QSCF-DC-DFT leads to a substantial improvement of DC-DFT methods in this case: The most stable T-til-AoB form is calculated to have a BSSE-corrected D_e value of -2.84 kcal/mol, in perfect agreement with the best CCSD(T) calculations. If the ZPE corrections is added a D_0 value of -2.40 kcal/mol is obtained that agrees with the most reliable experimental value of -2.40 ± 0.40 kcal/mol. All other dimer forms for which accurate CCSD(T) results are available show a similar convincing accuracy of QSCF-DC-DFT, thus providing evidence that the extensive PES investigation obtained in this work is reliable. We could describe seven rearrangement processes of the benzene dimer via the 16 stationary points involved in these processes. The PES is extremely flat in the direction of intracomplex rotations and certain parallel displacements of the two rings. If ZPE corrections are included, there is a further adjustment of binding energies. This leads to three important conclusions: (a) The D_0 values of the T-til-AoB and PD-AoA forms are identical at the QSCF-DC-DFT level of theory, suggesting that one can expect in the gas phase at low temperatures close to 0 K an equal population of the two forms. (b) Even at low temperature, the benzene dimer will undergo large-amplitude vibrations so that its structural determination by experimental means becomes extremely difficult. (c) With rising temperatures, energetic differences between the eight most stable benzene dimer forms will be annihilated.

The experiences from the investigation of the benzene dimer PES suggest that QSCF-DC-DFT is the appropriate method for routine investigations on dispersion stabilized complexes between aromatic molecules, DNA base pairs, molecules on graphene or CNTs and between CNTs in a rod.

ACKNOWLEDGMENTS

D.C. thanks the University of the Pacific for support.

[1] S. K. Burley and G. A. Petsko, Science **229**, 23 (1985).
[2] C. A. Hunter, J. Singh, and J. M. Thornton, J. Mol. Biol. **218**, 837 (1991).
[3] J.-Y. Ortholand, A. M. Z. Slawin, N. Spencer, J. F. Stoddart, and D. J. Williams, Angew. Chem., Int. Ed. Engl. **28**, 1394 (1989).
[4] E. A. Meyer, R. K. Castellano, and F. Diederich, Angew. Chem., Int. Ed. Engl. **42**, 1210 (2003).
[5] W. Saenger, *Principles of Nucleic Acid Structure* (Springer, New York, 1984).
[6] B. Askew, P. Ballester, C. Buhr, K. S. Jeong, K. Jones, K. Parris, K. Williams, and J. Rebek, J. Am. Chem. Soc. **111**, 1082 (1989).
[7] D. B. Smithrud and F. Diederich, J. Am. Chem. Soc. **112**, 339 (1990).
[8] C. A. Hunter, Chem. Soc. Rev. **23**, 101 (1994).
[9] J. Rebek, Jr., Chem. Soc. Rev. **25**, 255 (1996).
[10] P. J. F. Harris, *Carbon Nanotubes and Related Structures* (Cambridge University Press, Cambridge, 1999).
[11] L. S. Lerman, J. Mol. Biol. **3**, 18 (1961).
[12] M. F. Brana, M. Cacho, A. Gradillas, B. Pascual-Teresa, and A. Ramos, Curr. Pharm. Des. **7**, 1745 (2001).
[13] For a recent review see, S. Tsuzuki, in *Structure and Bonding* (Springer, Berlin, 2005), Vol. 115, pp. 149–193.
[14] K. C. Janda, J. C. Hemminger, J. S. Winn, S. E. Novick, S. J. Harris, and W. Klemperer, J. Chem. Phys. **63**, 1419 (1975).
[15] J. M. Steed, T. A. Dixon, and W. Klemperer, J. Chem. Phys. **70**, 4940 (1979).
[16] J. R. Grover, E. A. Walters, and E. T. Hui, J. Phys. Chem. **91**, 3233 (1987).
[17] H. Krause, B. Ernstberger, and H. J. Neusser, Chem. Phys. Lett. **184**, 411 (1991).
[18] B. F. Henson, G. V. Hartland, V. A. Venturo, and P. M. Felker, J. Chem. Phys. **97**, 2189 (1992).
[19] W. Scherzer, O. Kratzschmar, H. L. Selzle, and E. W. Schlag, Z. Naturforsch., A: Phys. Sci. **47**, 1248 (1992).
[20] E. Arunan and H. S. Gutowsky, J. Chem. Phys. **98**, 4294 (1993).
[21] U. Erlekam, M. Frankowski, G. Meijer, and G. von Helden, J. Chem. Phys. **124**, 171101 (2006).
[22] U. Erlekam, M. Frankowski, G. von Helden, and G. Meijer, Phys. Chem. Chem. Phys. **9**, 3786 (2007).
[23] S. Tsuzuki, T. Uchimaru, K. Matsumura, M. Mikami, and K. Tanabe, Chem. Phys. Lett. **319**, 547 (2000).
[24] S. Tsuzuki, K. Honda, T. Uchimaru, M. Mikami, and K. Tanabe, J. Am. Chem. Soc. **124**, 104 (2002).
[25] S. Tsuzuki, T. Uchimaru, K. Sugawara, and M. Mikami, J. Chem. Phys. **117**, 11216 (2002).
[26] M. O. Sinnokrot, E. V. Valeev, and C. D. Sherrill, J. Am. Chem. Soc. **124**, 10887 (2002).
[27] A. Reyes, M. A. Tlenkopatchev, L. Fomina, P. Guadarrama, and S. Fomine, J. Phys. Chem. A **107**, 7027 (2003).
[28] M. O. Sinnokrot and C. D. Sherrill, J. Phys. Chem. A **107**, 8377 (2003).
[29] M. O. Sinnokrot and C. D. Sherrill, J. Am. Chem. Soc. **126**, 7690 (2004).

[30] S. Tsuzuki, K. Honda, T. Uchimaru, and M. Mikami, J. Chem. Phys. **120**, 647 (2004).
[31] M. O. Sinnokrot and C. D. Sherrill, J. Phys. Chem. A **108**, 10200 (2004).
[32] T. Sato, T. Tsuneda, and K. Hirao, J. Chem. Phys. **123**, 104307 (2005).
[33] R. Podeszwa, R. Bukowski, and K. Szalewicz, J. Phys. Chem. A **110**, 10345 (2006).
[34] J. Grant Hill, J. A. Platts, and H.-J. Werner, Phys. Chem. Chem. Phys. **8**, 4072 (2006).
[35] M. O. Sinnokrot and C. D. Sherrill, J. Phys. Chem. A **110**, 10656 (2006).
[36] V. Spirko and P. Hobza, ChemPhysChem **7**, 640 (2006).
[37] P. Jurečka, J. Sponer, J. Cerny, and P. Hobza, Phys. Chem. Chem. Phys. **8**, 1985 (2006).
[38] R. A. DiStasio, Jr., G. von Helden, R. P. Steele, and M. Head-Gordon, Chem. Phys. Lett. **437**, 277 (2007).
[39] W. Z. Wang, M. Pitonak, and P. Hobza, ChemPhysChem **8**, 2107 (2007).
[40] T. Janowski and P. Pulay, Chem. Phys. Lett. **447**, 27 (2007).
[41] S. Grimme, J. Antony, T. Schwabe, and C. Mück-Lichtenfeld, Org. Biomol. Chem. **5**, 741 (2007).
[42] M. Swart, T. van der Wijst, C. Fonseca Guerra, and F. M. Bickelhaupt, J. Mol. Model. **13**, 1245 (2007).
[43] J. G. Hill and J. A. Platts, J. Chem. Theory Comput. **3**, 80 (2007).
[44] E. C. Lee, D. Kim, P. Jurecka, P. Tarakeshwar, P. Hobza, and K. S. Kim, J. Phys. Chem. A **111**, 3446 (2007).
[45] L. V. Slipchenko and M. S. Gordon, J. Comput. Chem. **28**, 276 (2007).
[46] S. Grimme, Angew. Chem., Int. Ed. **47**, 3430 (2008).
[47] O. Bludsky, M. Rubes, P. Soldan, and P. Nachtigall, J. Chem. Phys. **128**, 114102 (2008).
[48] W. Kohn, Y. Meir, and D. E. Makarov, Phys. Rev. Lett. **80**, 4153 (1998).
[49] Y. Andersson, D. C. Langreth, and B. I. Lundqvist, Phys. Rev. Lett. **76**, 102 (1996).
[50] M. Kamiya, T. Tsuneda, and K. Hirao, J. Chem. Phys. **117**, 6010 (2002).
[51] T. Sato, T. Tsuneda, and K. Hirao, Mol. Phys. **103**, 1151 (2005).
[52] T. Sato, T. Tsuneda, and K. Hirao, J. Chem. Phys. **126**, 234114 (2007).
[53] M. Dion, H. Rydberg, E. Schröder, D. C. Langreth, and B. I. Lundqvist, Phys. Rev. Lett. **92**, 246401 (2004); **95**, 109902 (2005).
[54] D. C. Langreth, M. Dion, H. Rydberg, E. Schröder, P. Hyldgaard, and B. I. Lundqvist, Int. J. Quantum Chem. **101**, 599 (2005).
[55] T. Thonhauser, V. R. Cooper, S. Li, A. Puzder, P. Hyldgaard, and D. C. Langreth, Phys. Rev. B **76**, 125112 (2007).
[56] A. Puzder, M. Dion, and D. C. Langreth, J. Chem. Phys. **124**, 164105 (2006).
[57] T. Thonhauser, A. Puzder, and D. C. Langreth, J. Chem. Phys. **124**, 164106 (2006).
[58] S. D. Chakarova and E. Schröder, J. Chem. Phys. **122**, 054102 (2005); S. Chakarova-Käck, E. Schröder, B. I. Lundqvist, and D. C. Langreth, Phys. Rev. Lett. **96**, 146107 (2006).
[59] O. Vydrov, Q. Wu, and T. Van Voorhis, J. Chem. Phys. **129**, 014106 (2008).
[60] I. C. Gerber and J. G. Ángyán, Chem. Phys. Lett. **416**, 370 (2005).
[61] J. G. Ángyán, I. C. Gerber, A. Savin, and J. Toulouse, Phys. Rev. A **72**, 012510 (2005).
[62] F. Furche and T. Van Voorhis, J. Chem. Phys. **122**, 164106 (2005).
[63] E. R. Johnson and A. D. Becke, J. Chem. Phys. **123**, 024101 (2005); **124**, 174104 (2006).
[64] A. D. Becke and E. R. Johnson, J. Chem. Phys. **127**, 124108 (2007).
[65] X. Xu and W. A. Goddard III, Proc. Natl. Acad. Sci. U.S.A. **101**, 2673 (2004).
[66] Y. Zhao and D. G. Truhlar, J. Phys. Chem. A **108**, 6908 (2004).
[67] Y. Zhao, N. E. Schultz, and D. G. Truhlar, J. Chem. Theory Comput. **2**, 364 (2006).
[68] I. V. Schweigert, V. F. Lotrich, and R. J. Bartlett, J. Chem. Phys. **125**, 104108 (2006).
[69] O. Gritsenko and E. J. Baerends, J. Chem. Phys. **124**, 054115 (2006).
[70] Y. Zhao and D. G. Truhlar, J. Chem. Theory Comput. **3**, 289 (2007).
[71] H. L. Williams and C. F. Chabalowski, J. Phys. Chem. A **105**, 646 (2001).
[72] A. Heßelmann and G. Jansen, Chem. Phys. Lett. **362**, 319 (2002).
[73] A. J. Misquitta and K. Szalewicz, Chem. Phys. Lett. **357**, 301 (2002).
[74] R. Podeszwa, R. Bukowski, and K. Szalewicz, J. Chem. Theory Comput. **2**, 400 (2006).
[75] M. Rubes, O. Bludsky, and P. Nachtigall, ChemPhysChem **9**, 1702 (2008).
[76] M. Elstner, P. Hobza, T. Frauenheim, S. Suhai, and E. Karixas, J. Chem. Phys. **114**, 5149 (2001).
[77] X. Wu, M. C. Vargas, S. Nayak, V. Lotrich, and G. Scoles, J. Chem. Phys. **115**, 8748 (2001).
[78] Q. Wu and W. Yang, J. Chem. Phys. **116**, 515 (2002).
[79] S. Grimme, J. Comput. Chem. **25**, 1463 (2004).
[80] S. Grimme, J. Comput. Chem. **27**, 1787 (2006).
[81] M. Pavone, N. Rega, and V. Barone, Chem. Phys. Lett. **452**, 333 (2008).
[82] S. Kristyan and P. Pulay, Chem. Phys. Lett. **229**, 175 (1994).
[83] P. Hobza, J. Sponer, and T. Reschel, J. Comput. Chem. **16**, 1315 (1995).
[84] J. M. Pérez-Jordá and A. D. Becke, Chem. Phys. Lett. **233**, 134 (1995).
[85] I. Panas, Chem. Phys. Lett. **245**, 171 (1995).
[86] T. Leininger, H. Stoll, H.-J. Werner, and A. Savin, Chem. Phys. Lett. **275**, 151 (1997).
[87] R. D. Adamson, J. P. Dombroski, and P. M. W. Gill, J. Comput. Chem. **20**, 921 (1999).
[88] A. Tkatchenko and O. A. von Lilienfeld, Phys. Rev. B **78**, 045116 (2008).
[89] S. Grimme, J. Chem. Phys. **124**, 034108 (2006).
[90] O. A. von Lilienfeld, I. Tavernelli, U. Röthlisberger, and D. Sebastiani, Phys. Rev. Lett. **93**, 153004 (2004); I.-C. Lin, M. D. Coutinho-Neto, C. Felsenheimer, O. A. von Lilienfeld, I. Tavernelli, and U. Röthlisberger, Phys. Rev. B **75**, 205131 (2007).
[91] G. A. DiLabio, Chem. Phys. Lett. **455**, 348 (2008).
[92] E. Engel, A. Hoeck, and R. M. Dreizler, Phys. Rev. A **61**, 032502 (2000).
[93] J. D. Talman and W. F. Shadwick, Phys. Rev. A **14**, 36 (1976).
[94] A. Görling and M. Levy, Phys. Rev. A **50**, 196 (1994).
[95] For a review, see D. Cremer, in *Encyclopedia of Computational Chemistry*, edited by P. v. R. Schleyer, N. L. Allinger, T. Clark, J. Gasteiger, P. A. Kollman, H. F. Schaefer, and P. Schreiner (Wiley, Chichester, UK, 1998), Vol. 3, p. 1706.
[96] S. Grimme, J. Chem. Phys. **118**, 9095 (2003); J. Comput. Chem. **24**, 1529 (2003).
[97] B. W. Hopkins and G. S. Tschumper, J. Phys. Chem. A **108**, 2941 (2004).
[98] P. Hobza, *Accurate Interaction Energies of Building Blocks of Biomacromolecules: A Quantum Chemical Study* (WATOC 8, Sydney, Australia, 2008).
[99] J. P. Perdew, K. Burke, and M. Ernzerhof, Phys. Rev. Lett. **77**, 3865 (1996).
[100] A. D. Becke, Phys. Rev. A **38**, 3098 (1988).
[101] C. Lee, W. Yang, and R. P. Parr, Phys. Rev. B **37**, 785 (1988).
[102] T. Tsuneda, T. Suzumura, and K. Hirao, J. Chem. Phys. **110**, 10664 (1999).
[103] Y. Zhang and W. Yang, Phys. Rev. Lett. **80**, 890 (1998).
[104] J. Toulouse, F. Colonna, and A. Savin, J. Chem. Phys. **122**, 014110 (2005).
[105] E. B. J. Wilson, J. C. Decius, and P. C. Cross, *Molecular Vibrations, The Theory of Infrared and Raman Vibrational Spectroscopy* (McGraw-Hill, London, 1955).
[106] C. Peng, P. Y. Ayala, H. B. Schlegel, and M. J. Frisch, J. Comput. Chem. **17**, 49 (1996).
[107] E. Kraka, J. Gräfenstein, M. Filatov, H. Joo, D. Izotov, J. Gauss, Y. He, A. Wu, V. Polo, L. Olsson, Z. Konkoli, Z. He, and D. Cremer, COLOGNE08, University of the Pacific, Stockton CA, 2008.
[108] E. Stratmann, G. E. Scuseria, and M. J. Frisch, Chem. Phys. Lett. **257**, 213 (1996).
[109] R. F. W. Bader, *Atoms in Molecules, A Quantum Theory* (Clarendon, Oxford, 1990).
[110] T. H. Dunning, Jr., J. Chem. Phys. **90**, 1007 (1989).
[111] S. F. Boys and F. Bernardi, Mol. Phys. **19**, 553 (1970).
[112] J.-P. Ryckaert, G. Ciccotti, and H. J. C. Berendsen, J. Comput. Phys. **23**, 327 (1977).
[113] D. Cremer and J. A. Pople, J. Am. Chem. Soc. **97**, 1354 (1975).
[114] D. Cremer and D. Izotov (unpublished).